14th AMS Aviation, Range and Aerospace Conference, 17-21 Jan 2010, Atlanta, GA

Improvements to an Operational Clear Air Turbulence Diagnostic Index

GARY P. ELLROD [1]
NOAA/NESDIS (Retired)
Granby, CT

JOHN A. KNOX
Department of Geography, University of Georgia,
Athens, GA

1. Introduction

During the past four decades, various indices have been developed to help diagnose and forecast the likelihood of high altitude clear-air turbulence (CAT) near the jet stream (e.g., Endlich 1964; Brown 1973; Lee et al. 1984; Ellrod and Knapp 1992; Kaplan et al. 2005). These forecast indices are typically based on variables derived from upper-air observations or numerical weather prediction (NWP) model data. A more recent statistical approach that uses a continually updated, weighted regression of ten of these diagnostics is known as Graphical Turbulence Guidance-2 (GTG2) (Sharman et al. 2006). The diagnostics used in GTG2 have consistently provided the best overall performance. At a typical aviation forecast center today, forecasters employ a "toolbox" consisting of many, if not all, of these turbulence diagnostic indices individually, as well as combined within GTG2, along with real-time PIREPs.

CAT indices based on NWP or upper air data attempt to capture grid-scale processes that produce the mesoscale (10-100 km) meteorological conditions conducive to sub-grid-scale turbulence that affects aircraft. In addition to problems related to scale, many of the indices account for some, but not all, of the CAT-producing mechanisms in some, but not all, circumstances. For example, most do not account for turbulence initiated by mountain waves. Then there is the long-noted connection between upper-level ridges and CAT (e.g., Lester 1994). Knox (1997) drew attention to problems with the application of various CAT indices in strongly anticyclonic flows. In such situations, deformation-based diagnostics (e.g., Brown 1973; Ellrod and Knapp 1992) may wrongly predict CAT, or correctly predict it for the wrong reasons, by relating deformation to frontogenesis. Also, Knox (1997) demonstrated that in pronounced anticyclonic horizontal shear and curvature, the ageostrophic vertical wind shear is additive with the geostrophic vertical wind shear, leading to large shears in ridges and therefore greater probabilities of Kelvin-Helmholtz instability (KHI). In the very strongest anticyclonic situations, CAT may also be related to inertial instability (Knox 2003) and/or gravity wave generation by this instability (O'Sullivan 1993).

Taken together, the results of Knox's (1997) analysis indicated that deformation-based diagnostics could be improved by incorporating a parameter appropriate for the dynamics of anticyclonic flow. One such parameter is divergence tendency, which is often large in two circumstances related to CAT: strong ridges, as well as cyclonic regions that are not in quasi-geostrophic (QG)

[1] *Corresponding author address*: Gary P. Ellrod, P.O. Box 240, Granby, CT, Email: gary.ellrod@gmail.com

or gradient balance. Based a scale analysis of the Lighthill-Ford theory of spontaneous imbalance, Knox et al. (2008) provided a physical link between deformation and divergence tendency in spontaneous gravity wave generation favorable for CAT. In an evaluation of six CAT diagnostic parameters, McCann (2001) found the highest correlation between divergence tendency and CAT among six parameters evaluated. These findings may explain why deformation-based diagnostics such as TI can succeed even in non-frontogenetical situations, by accounting for regions of gravity wave generation.

This paper describes efforts to improve an existing and widely-used CAT diagnostic index, the Turbulence Index (TI) of Ellrod and Knapp (1992). Versions of TI have been implemented by operational aviation forecast units globally, including the National Oceanic and Atmospheric Administration (NOAA) Aviation Weather Center (AWC) (Behn 2008), the Air Force Weather Agency (Brooks and Oder 2004), the Meteorological Office in the United Kingdom (Turp and Gill 2008) and the Canadian Meteorological Centre (Turcotte and Verret 1999). TI is also one of the ten diagnostic indices used by GTG2 (Sharman et al. 2006). TI is popular because of its good performance (Brown et al. 2000), familiarity among forecasters, its computational speed and easy implementation. In light of shortcomings described previously however, a more universal and robust diagnostic index is desired. The proposed change to TI is to add a proxy term for divergence tendency to account for CAT in situations of rapidly changing divergence associated with anticyclonic flow (both shear and curvature), and in cyclonic regions not in gradient balance. In Section 2 we describe DTI and the method used to identify improvements versus the earlier version of the index (TI). In Section 3, an example is shown using data from a mesoscale numerical model that demonstrates how DTI could have improved the anticipation of significant turbulence in an operational setting. In Section 4, we provide verification statistics for two separate one-month periods (July and December 2007). Section 5 summarizes the results and discusses the operational utility of the new DTI diagnostic.

2. Data and procedures

The index used as a basis for the experiments was TI, more specifically TI1 in Equation 9 in Ellrod and Knapp (1992). TI is defined as:

$$TI = [(\Delta u/\Delta x - \Delta v/\Delta y)^2 + (\Delta v/\Delta x + \Delta u/\Delta y)^2]^{1/2} (\Delta V/\Delta z) \quad (2)$$

A B

Term A is resultant deformation (DEF), and B is vertical wind shear (VWS) of the total vector wind V at each grid point.

To improve TI by accounting for rapidly changing divergent flows, a simplified "divergence trend" term (DVT) was obtained, defined as:

$$DVT = C [(\Delta u/\Delta x + \Delta v/\Delta y)_{h2} - (\Delta u/\Delta x + \Delta v/\Delta y)_{h1}] \quad (3)$$

DVG_2 DVG_1

The subscripts h1 and h2 represent the two forecast intervals used in determining DVT. In order to evaluate the feasibility of this approach, 6-hr, 12-hr, or 18-hr forecast times were used initially for the North American Mesoscale (NAM) (Rogers et al. 2005), and the Global Forecast System (GFS) (Global Climate and Weather Modeling Branch 2003) models. For the latest version of the Rapid Update Cycle (RUC2) (Benjamin et al. 2003), the 3-hr and 6-hr forecast times were used. C is a constant; its value was subjectively assigned as 0.1 to allow DVT to be roughly equivalent in magnitude to the deformation-

shear term in TI in situations where large changes in divergence are present. (Divergence tendency is typically too small to make an impact on TI). The same value of C was used for all models, which did not permit inter-comparison of those results. In future evaluations, C will be proportional to the time interval.

The DVT was then added to TI to create the Divergence-modified Turbulence Index DTI:

$$DTI = TI + DVT \quad (4)$$

TI and DTI data were generated on a Man-computer Interactive Data Access System (McIDAS) workstation at the National Environmental Satellite, Data and Information Service' (NESDIS) Center for Satellite Applications Research (STAR). The model data were obtained from the NOAA National Centers for Environmental Prediction (NCEP) in Camp Springs, Maryland. TI and DTI were produced mainly for the 300 hPa to 250 hPa layer, corresponding to flight altitudes of approximately 30,000-34,000 ft (9.2 – 10.4 km) above Mean Sea Level (MSL). Pseudo-color images of TI and DTI were made available on the Web at: http://www.star.nesdis.noaa.gov/smcd/opdb/aviation/turb/tifcsts.html

3. Example: 25 May 2005

The 250 hPa conditions for 1200 UTC, 25 May 2005 (Fig. 1) revealed a sharply defined short-wave trough-ridge couplet over the Upper Midwest, extending into the northern Great Lakes region. Farther east, a closed upper low was entrenched over the Northeastern United States, but moving slowly eastward away from the Mid-Atlantic Coast. A strong jet with maximum winds of 105 kt at the base of the short-wave trough was observed at Rapid City, SD (RAP). In advance of the jet, diffluent/divergent flow could be seen in the exit region, creating a region of possible strong gravity wave generation toward the ridge axis, which extended from northern Michigan to southeast Iowa.

Figure 2 compares the 18hr forecast NAM TI (a) and DTI (b) output valid at 1200 UTC, 25 May 2005. Both showed a maximum value in the northern Great Lakes due to the deformation and vertical wind shear near the ridge axis. DTI showed a second maximum over northwest Wisconsin to southern Minnesota which was due to the increase in upper divergence that had occurred in the prior six hour period in advance of the jet maximum in South Dakota. The PIREPs for the 0900 UTC-1500 UTC period (Fig. 2) indicated considerable moderate or greater turbulence in this region. Aside from the DTI maximum in southwest Minnesota, there were only minor differences between the two indices elsewhere.

A GOES water vapor image at 1215 UTC 25 May 2005 is shown in Fig 3. Embedded convection is evident over Iowa and southwest Minnesota, with extensive transverse banding present in the cloud tops. Transverse cloud bands are usually a good indicator of high altitude turbulence (Ellrod 1985; Knox et al. 2009). The 1204 UTC radar display from Minneapolis (KMSP) (Fig. 4) indicated that two of the moderate or greater turbulence reports in southern Minnesota were likely associated with the convection. However, there were also numerous reports of light-moderate "chop" by aircraft approaching or departing Minneapolis-St. Paul (MSP) from/to the east at altitudes of FL290 or lower, confirming a high threat for CAT associated with the southern DTI maximum. Radar showed no significant convection in this area.

4. Verification

a. Data and procedures

Verification was accomplished by comparing PIREP turbulence intensity with RUC2 model grid point values of the 6-hr forecast of both DTI and the legacy TI for the 250 hPa – 300 hPa layer. Data was collected for occurrences of light-to-moderate or greater turbulence intensity, and also for null (smooth) occurrences over the eastern two-thirds of the United States within $\pm$ 1 hr of the forecast valid time. The data were obtained during two separate periods: (1) 26 June to 31 July 2007 (hereafter, July 2007), and (2) December 2007, for a total of 1,168 forecast/observation pairs for each index. The July 2007 data were screened to eliminate turbulence possibly related to convection by using low resolution WSR-88D radar images available from the NOAA National Climatic Data Center. The index value nearest the turbulence report was used for each data pair. Some manual interpolation was required in regions of strong gradients. Negative grid point values were rounded up to zero, and assumed to represent non-turbulent conditions.

Verification metrics such as Probability of Detection of both turbulent (POD_y) and smooth conditions (POD_n), and True Skill Statistic ($TSS = POD_y + POD_n - 1$) were then produced and compared for the two algorithms using various index thresholds (0, 1, 2, 4, 6, 8, 10, 12, and 16) as turbulence discriminators. The TSS measures the ability of a diagnostic index to discriminate between 'yes' and 'no' turbulence forecasts. Common verification metrics such as False Alarm Rate (FAR), Critical Success Index (CSI), and Bias are not considered to be appropriate for use with PIREPs since their values change as the number of yes or no PIREPs changes (Brown and Young 2000). Plots of POD_y versus $1 - POD_n$ for all thresholds were used to create a Relative Operating Characteristic (ROC) diagram (Mason and Graham 1999). ROC curves allow a user to determine the optimum threshold value of an index that results in the best POD_y with a corresponding acceptably low value of $1 - POD_n$.

b. Results

Table 1 shows values of POD_y, POD_n, and TSS for both DTI and TI algorithms for July 2007, December 2007, and both months combined using a threshold value of '4' as a discriminator between turbulent and smooth conditions. This threshold value is the one typically used in operational forecasts. For the combined data set, the improvement in DTI over TI is approximately 50% for POD_y, and is better by a factor of five for TSS. POD_n was slightly worse for DTI for all three data sets, suggesting that DTI over-forecasts turbulence slightly relative to TI. Relative improvements for other threshold values (not shown) were similar, although the best verification metrics for DTI (based on the TSS value) were obtained using the threshold value of '4.' The results for December 2007 were better for DTI than for July 2007, although the latter was a much smaller data set.

A ROC diagram comparing DTI, TI, and the operational GTG2 for December, 2007 is shown in Figure 5. (GTG2 data were obtained from NOAA Earth System Resource Laboratory's Real-time Verification System at: http://rtvs.noaa.gov/turb/op/stats/index.html) The area between the DTI curve and the diagonal line (representing the amount of skill) is larger than that of the TI, showing that the addition of the proxy for divergence tendency has improved the performance of the original TI, which was the primary goal of this verification effort.

Figure 5 also shows that performance of GTG2 for December 2007 was superior to DTI. GTG2 contained a much larger number of reports than for the DTI/TI data set, due to

a deeper atmospheric layer (FL200-400 versus FL290-340 for DTI/TI), and a wider domain (Continental U. S. versus eastern half of CONUS). Previous studies comparing an earlier version of GTG with TI found the two metrics to have comparable validity (e.g. Brown et al. 2000). For these reasons, we feel that the verification results for DTI cannot be fairly compared to GTG2 and are shown for informational purposes only.

Despite apparent issues with the size and quality of the pilot report data base, our results clearly show that DTI is a significant improvement upon TI and will be a valuable upgrade to existing operational forecast diagnostic tools, as well as a likely contribution to improved performance of the operational GTG2. A more extensive verification study of the DTI and other algorithms is planned at the Aviation Weather Center beginning late 2009 through 2011, using data from additional state-of-the-art prediction models, altitude ranges, and forecast times (Knox et al. 2010).

5. Summary and operational utility

Based on qualitative comparisons, and two months of quantitative verification (using parameters such as POD_y, POD_n and TSS), we conclude that maxima of the Turbulence Index (TI) in anticyclonic shear and/or curvature associated with upper ridges, and even in cyclonic flow situations in the exit region of strong jets were enhanced considerably by the additions of a divergence trend (DVT) term. The resulting algorithm is what we call the Divergence-modified Turbulence Index (DTI) diagnostic. The DTI related better spatially with turbulence reports than did TI. On many days, there were only minor differences between the DTI and TI anywhere within the domain of the CONUS and southern Canada. This would be expected in light of the relative rarity of the large divergence changes we are attempting to highlight. We encourage the evaluation of the DTI algorithm at aviation forecast centers to determine if implementation would bring improvements to their operational turbulence forecasts. Further evaluations of this DTI at AWC will begin during winter 2009-10 using state-of-the-art models at varying time intervals in an effort to obtain maximum benefits from this new diagnostic index. Details of this research are provided in Knox et al. (2010).

Acknowledgments: The authors would like to thank Andrew Bailey (IM Systems Group, Camp Springs, MD) for modifications to the existing turbulence index code, Kenneth Pryor, aviation project manager at NOAA/NESDIS Center for Satellite Applications and Research, and Ankita Nagirimadugu, who obtained the summer 2007 verification statistics.

REFERENCES

Behn, D., 2008: NAM-WRF Verification of subtropical jet turbulence, National Weather Association *Electronic Journal of Operational Meteorology*, paper 2008-EJ3.

Benjamin, S. G., D. Devenyi, S.S. Weygandt, K.J. Brundage, J.M. Brown, G.A. Grell, D. Kim, B.E. Schwartz, T.G. Smirnova, T.L. Smith, and G.S. Manikin, 2003: An hourly assimilation/forecast cycle: The RUC. *Mon. Wea. Rev.* ,**132**, 495-518.

Brooks, G. R., and A. Oder, 2004: Low-level turbulence algorithm testing at-or-below 10,000 ft. *Proceedings, 11th AMS conf. on Aviation, Range, and Aerospace Meteorology*, 4-7 October 2004, Hyannis, MA, Amer. Meteor. Soc., Boston.

Brown, B. G., and G. S. Young, 2000: Verification of icing and icing forecasts: Why some verification statistics can't be computed using PIREPs. *Preprints, 9th Conference on Aviation, Range, and Aerospace Meteorology*, Orlando, FL, 11-15 Sept., Amer. Meteor. Soc., Boston, 393-398.

_____, J. L. Mahoney, J. Henderson, T. L. Kane, R. Bullock, and J. E. Hart, 2000: The turbulence algorithm intercomparison exercise: Statistical verification results. Preprints, *Ninth Conf. on Aviation, Range, and Aerospace Meteorology*, Orlando, FL, Amer. Meteor. Soc., 466-471.

Brown, R., 1973: New indices to locate clear-air turbulence. *Meteorol. Mag.*, **102**, 347-361.

Ellrod, G. P., 1985: Detection of high level turbulence using satellite imagery and upper air data. NOAA Tech. Memo. NESDIS 10, U. S. Dept. of Commerce, Washington, DC, 30 pp.

_____, and D. I. Knapp, 1992: An objective clear-air turbulence forecasting technique: Verification and operational use. *Wea. Forecasting*, **7**, 150-165.

Endlich, R. M., 1964: The mesoscale structure of some regions of clear-air turbulence. *J. Appl. Meteor.*, **3**, 261-276.

Global Climate and Weather Modeling Branch, EMC, 2003: The GFS Atmospheric Model, *National Center for Environmental Prediction Office Note 442*, November 2003, available at: http://www.emc.ncep.noaa.gov/officenotes/newernotes/on442.pdf.

Kaplan, M. L., A. W. Huffman, K. M. Lux, J. D. Cetola, J. J. Charney, A. J. Riordan, Y.-L. Lin, and K. T. Wright, 2005: Characterizing the severe turbulence environments associated with commercial aviation accidents. Part 2: Hydrostatic mesoscale numerical simulations of supergradient wind flow and streamwise ageostrophic frontogenesis. *Meteorol. Atmos. Phys.*, **88**, 153-173.

Knox, J. A., 1997: Possible mechanisms of clear-air turbulence in strongly anticyclonic flow. *Mon. Wea. Rev.*, **125**, 1251-1259.

_____, 2003: Inertial instability. In *Encyclopedia of the Atmospheric Sciences*, eds. J. R. Holton, J. Pyle, and J. A. Curry, Academic Press, New York, 1004-1013.

_____, and V. L. Harvey, 2005: Global climatology of inertial instability and Rossby wave breaking in the stratosphere. *J. Geophys. Res.*, **110**, 10.1029/2004JD005068.

_____, D. W. McCann, and P. D. Williams, 2008: Application of the Lighthill-Ford theory of spontaneous imbalance to clear-air turbulence forecasting. *J. Atmos. Sci.*, **65**, 3292-3304. doi: 10.1175/2008JAS2477.1

_____, A. S. Bachmeier, W. M. Carter, J. E. Tarantino, L. C. Paulik, E. N. Wilson, G. S. Bechdol, and M. J. Mays, 2009: Transverse cirrus bands in weather systems: A grand tour of an enduring enigma. *Weather*, in press.

_____, G. P. Ellrod, and S. Silberberg, 2010: Improving forecasts of clear-air turbulence at NOAA's Aviation Weather Center with state-of-the-art diagnostics. *14th AMS Conf. on Aviation, Range, and Aerospace Meteorology*, 17-21 January 2010, Atlanta, GA, Amer. Meteor. Soc., Boston.

Lee, D. R., R. S. Stull, and W. S. Irvine, 1984: Clear air turbulence forecasting techniques. Air Weather Service Tech. Note AFGWC/TN-79/001 (REV), Air Force Global Weather Central, Offutt AFB, Nebraska, 16 pp.

Lester, P. F., 1994: *Turbulence: A New Perspective for Pilots*. Jeppesen, 275 pp.

Mason, S. J. and N. E. Graham, 1999: Conditional probabilities, relative operating characteristics, and relative operating levels. *Wea. Forecasting*, **14**, 713-725.

McCann, D. W., 2001: Gravity waves, unbalanced flow, and clear air turbulence. *Nat. Wea. Digest*, **25(1,2)**, 3-14.

O'Sullivan, D. J., 1993: Inertial instability and inertia–gravity wave generation in the midlatitude winter stratosphere. Preprints, *Ninth Conf. on Atmospheric and Oceanic Waves and Stability*, San Antonio, TX, Amer. Meteor. Soc., 96–97.

Sharman, R., C. Tebaldi, G. Wiener, and J. Wolff, 2006: An integrated approach to mid- and upper-level turbulence forecasting. *Wea. Forecasting*, **21**, 268-287.

Turcotte, M-F, and R. Verret, 1999: In-flight icing and turbulence forecasts for aviation. Proceedings, *6th Workshop on Operational Meteorology*, Halifax, Nova Scotia, 53-56.

Turp, D., and P. Gill, 2008: Developments in numerical clear air turbulence forecasting at the U.K. Met Office, *Proc. AMS 13th Conf. on Aviation, Range and Aerospace Meteorology*, 20-24 January 2008, New Orleans, LA, Amer. Meteor. Soc., Boston.

TABLE 1.

Verification of DTI vs. TI for July 2007, December 2007 and Both Months (Threshold = ≥4)

	July 2007 N=335		**December 2007** N=833		**Combined** N=1168	
	TI	**DTI**	**TI**	**DTI**	**TI**	**DTI**
PODy	0.220	0.349	0.321	0.474	0.284	0.421
PODn	0.887	0.775	0.706	0.678	0.736	0.692
TSS	0.107	0.123	0.027	0.152	0.020	0.113

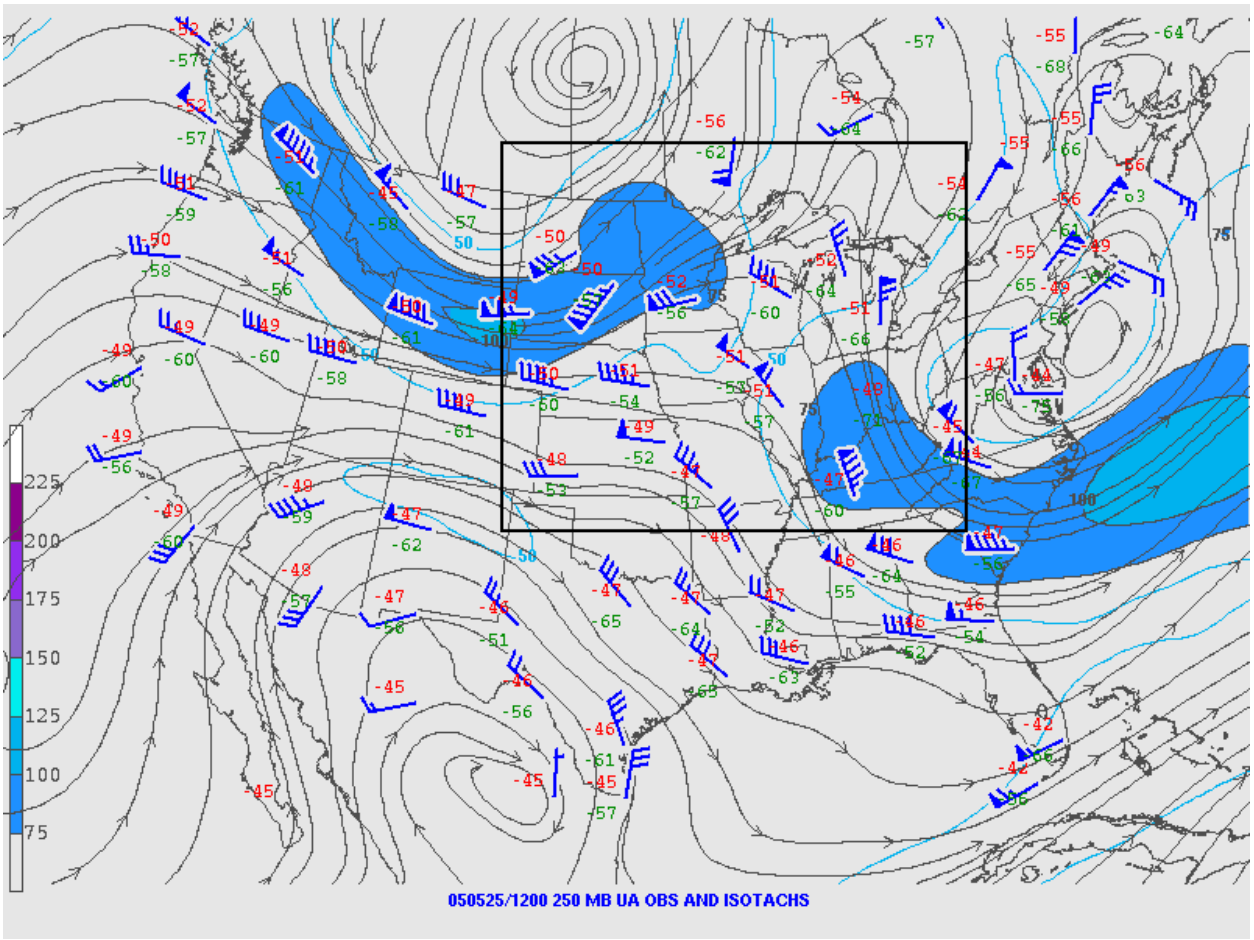

Figure 1: 250 hPa analysis valid at 1200 UTC, 25 May 2005. Black contours with arrows represent streamlines. Plotted winds are in knots (kt), with isotachs in blue. Winds greater than 75 kt are shaded. (Source: NOAA SPC)

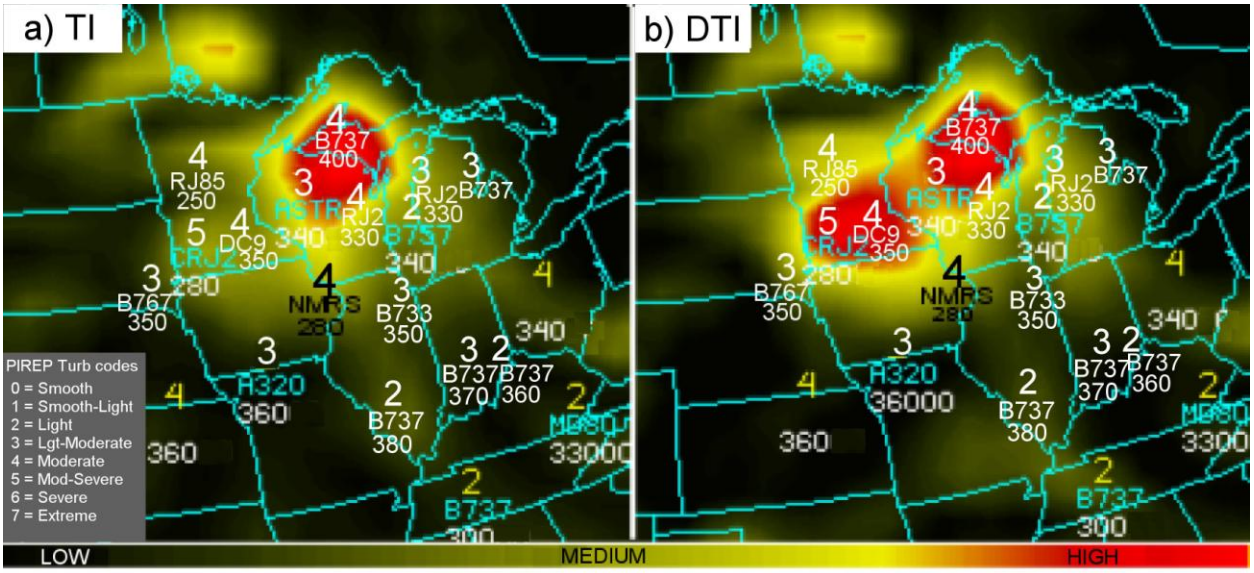

Figure 2: Image showing 12 hr NAM forecast of (a) TI and (b) DTI valid 1200 UTC, 25 May 2005. Yellow regions indicate medium risk of CAT; red areas indicate a high risk of CAT (TI or DTI >10). PIREP turbulence codes (scale at lower left), aircraft type, and altitude (100's of ft) were from 0900-1500 UTC.

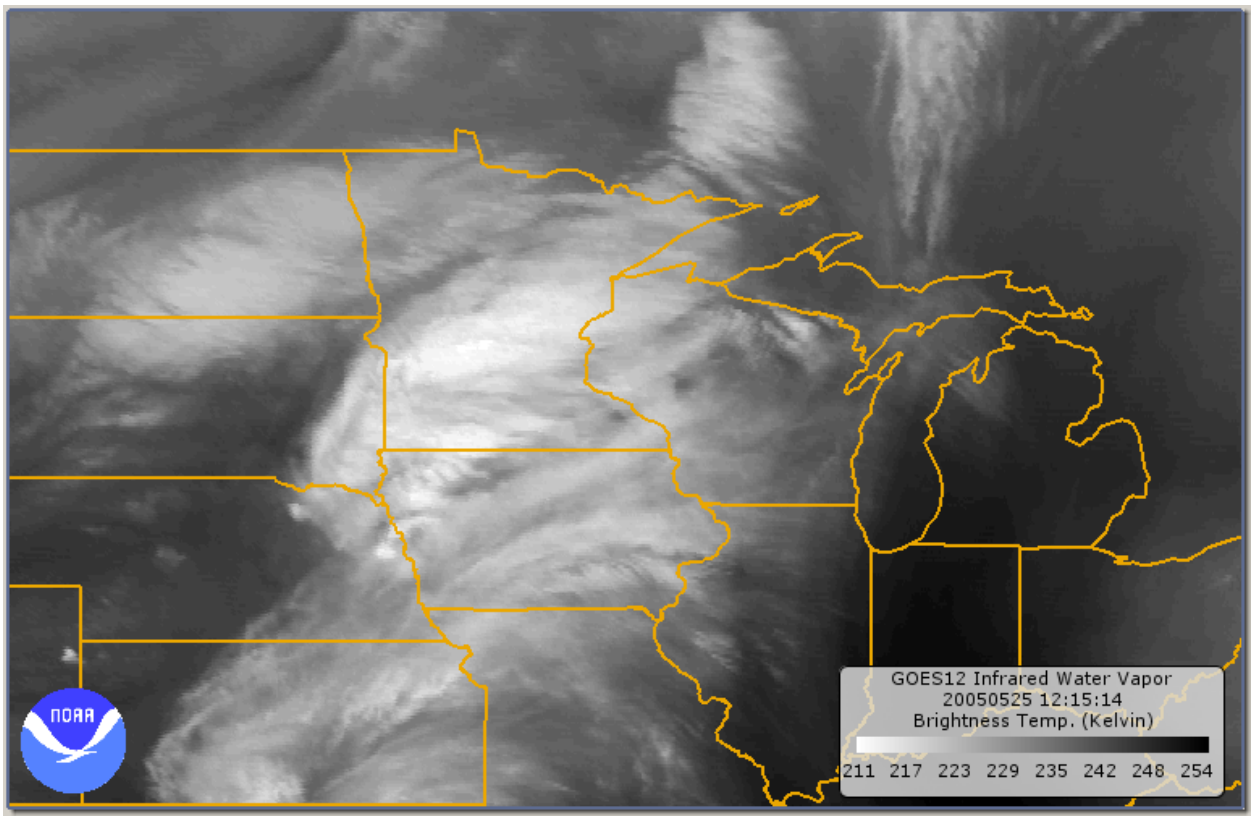

Figure 3: GOES-12 water vapor image at 1215 UTC, 25 May 2005. (Source: NOAA NCDC)

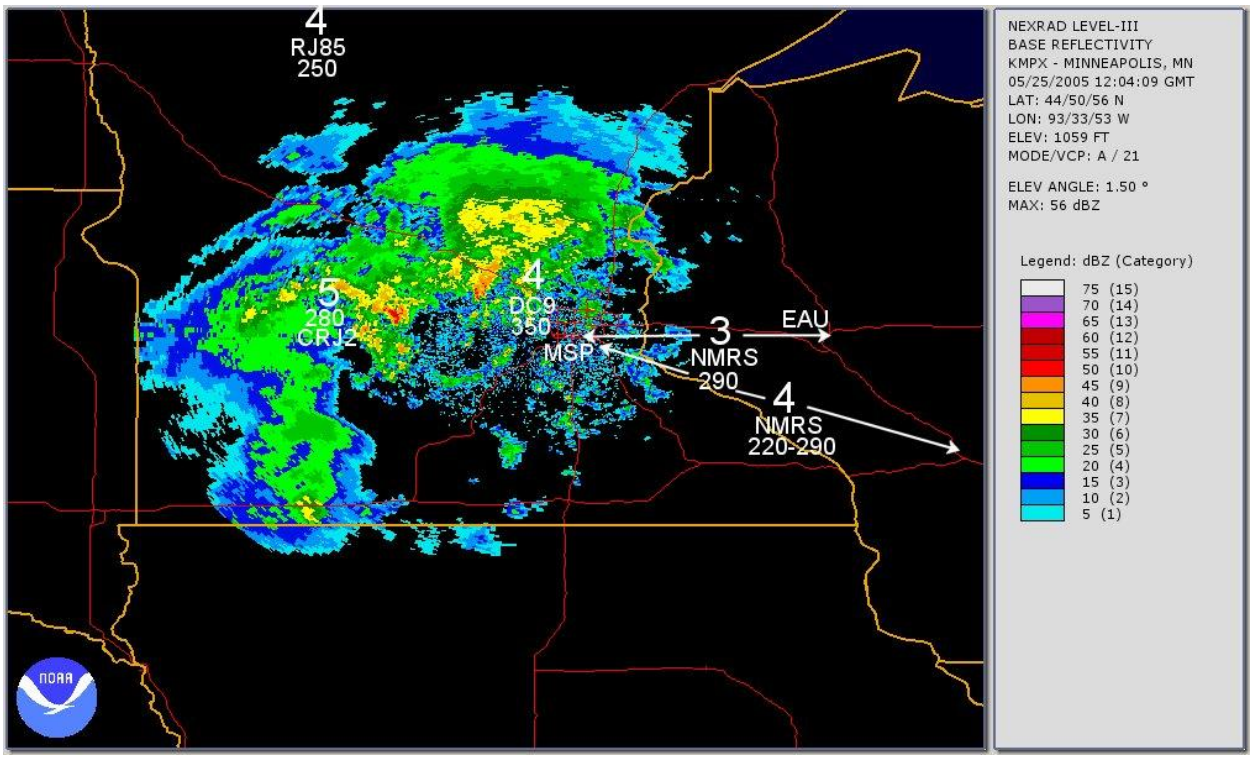

Figure 4: Radar reflectivity image from Minneapolis, MN (KMSP) at 1204 UTC, 25 May 2005 with turbulence reports ±1hr overlaid. Arrowed line segments show routes for numerous (NMRS) turbulence reports approaching/departing KMSP during this time. (Source: NOAA/NCDC)

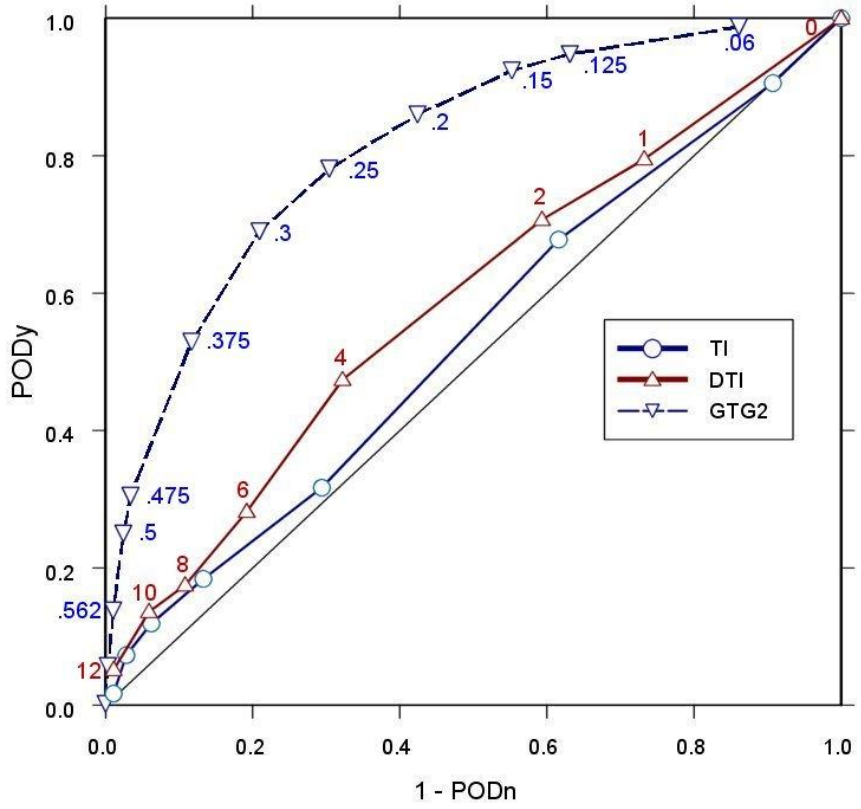

Figure 5: A diagram of Relative Operating Characteristics (ROC) for the DTI (red line, open triangles), TI (blue line, open circles), and (for informational purposes) GTG2 (dashed blue line, inverted open triangles) for December 2007. TI and DTI were obtained for FL290-340 in the eastern and central United States, while GTG2 data was for FL200-400 over the entire CONUS. Threshold values for DTI and GTG2 are shown.